
Nonadiabatic pumping in classical and quantum chaotic scatterers

A. CASTAÑEDA¹, T. DITTRICH^{2,3} and G. SINUCO⁴

¹ *Max Planck Institute of Microstructure Physics, Halle/Saale, Germany*

² *Departamento de Física, Universidad Nacional de Colombia, Bogotá D.C., Colombia*

³ *CeiBA – Complejidad, Bogotá D.C., Colombia*

⁴ *Department of Physics and Astronomy, University of Sussex, Brighton, UK*

PACS 05.45.-a – Nonlinear dynamics and chaos

PACS 05.60.-k – Transport processes

PACS 72.20.Dp – General theory, scattering mechanisms

Abstract. - We present a study of directed transport in periodically forced scattering systems in the regime of fast and strong driving where the dynamics is mixed to chaotic and adiabatic approximations do not apply. The model employed is a square potential well undergoing lateral oscillations, equivalent to an external AC voltage, alternatively as two-parameter and as single-parameter driving. On the classical level, mechanisms of directed transport are analyzed in terms of asymmetric irregular scattering processes. Quantizing the systems in the framework of Floquet scattering theory, we calculate directed currents on basis of transmission and reflection probabilities determined by numerical wavepacket scattering. We observe classical as well as quantum transport beyond linear response, manifest in particular in the case of single-parameter driving where according to adiabatic theory, currents would vanish identically.

Introduction. – The concept of pumping in nanosystems [1] has emerged from the paradigm of peristaltic pumps, simple idealized devices moving mass and/or charge in a defined direction as two or more parameters are cycled through a closed path [2]. As long as the driving is considered slow, adiabatic approximations apply. The idea has proven enormously fruitful, allowing for a very general analytical treatment involving quantum scattering theory and Berry phases [3–6], and has inspired a wide range of experimental realizations, including in particular solid-state systems such as semiconductor nanostructures, e.g., quantum dots driven by time-dependent gate voltages [7,8], and more recently graphene sheets [9,10]. These implementations, in turn, have stimulated the extension of theoretical approaches towards quantum pumps with fast and strong driving, leaving the adiabatic regime—largely equivalent to linear response [6]—far behind [11–13], as well as towards various many-body effects like dissipation and charge blocking.

By contrast, aspects of complex dynamics involved in directed transport in pumps have not yet been explored in depth. From the point of view of ballistic classical motion, peristaltic pumping corresponds to a trivial dynamics of the transported particles, moving phase-space

volumes through the device without mixing, much like a viscous liquid [4,6,14,15]. As sufficiently coherent and controllable sources of ever faster drivings become available, approaching the THz regime [16], pumping in the realm of nonadiabatic and strongly nonlinear dynamics comes within reach. Scattering theory, already at the heart of quantum pumping, provides us with an appropriate theoretical framework which by now has developed far beyond the adiabatic regime: Irregular scattering [17] is a mature field with numerous applications from celestial mechanics [18] down to chemical reactions [19–21], comprising classical as well as quantum phenomena and approaches.

With this work, we attempt a first survey into pumps operating in the regime of chaotic scattering and to give an overview of their principal features. As concerns implications of nonlinear dynamics induced by fast and strong forcing for directed transport, there exists a pertinent case already well studied: The concept of chaotic ratchets [22], in particular classical Hamiltonian ratchets amenable to direct quantization [23,24], has stimulated important insights into conditions and mechanisms of directed transport in this regime and its quantum manifestations. Similarly, starting from a comparable basis of results available on scattering at strongly driven potentials [25,26],

we will point out peculiarities of pumping due to a complex dynamics, such as currents manifestly violating linear response [27] and the possibility to achieve transport with a single driven parameter [13]. Conversely, the field of irregular scattering is being enriched by considerations around symmetry breaking [28] and finds new applications with significant technological perspectives [29]. Focusing on dynamical aspects, we however abstain from considering many-body phenomena in this work.

In the first, classical part of the paper, we devise a family of elementary one-dimensional models, composed of square potential wells which allow for two- as well as single-parameter driving, and analyze directed transport in these systems in terms of phase-space structures. The quantum part briefly introduces Floquet scattering theory as basic theoretical tool and provides numerical evidence, obtained from wavepacket scattering, for directed currents largely owing to the complex underlying classical motion. The concluding section provides an outlook to a number of questions left open by our work.

Classical chaotic pumps. –

Models. We seek models that (i) show irregular scattering, (ii) exhibit directed currents yet (iii) remain simple enough to permit an efficient numerical or even an analytical treatment, and (iv) are amenable to experimental realizations. Square potential wells and combinations of them almost ideally meet these conditions [25–27]: They allow for different types of external driving to induce chaotic behaviour and break symmetries as necessary to achieve directed transport, and they closely resemble the potentials of semiconductor superlattices in the transverse direction.

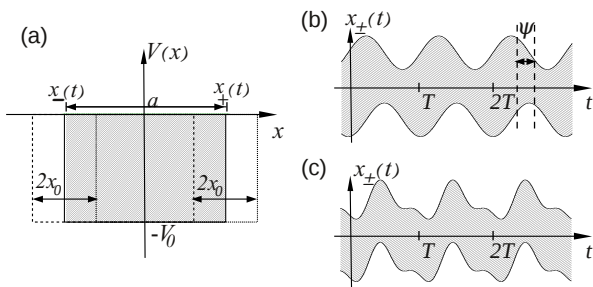


Fig. 1: Models for single- and two-parameter driving. Panel a: Laterally driven square potential well as in eq. (1); b: position of the potential well (shaded) as a function of time for two-parameter driving, eq. (2); c: same for single-parameter driving, eqs. (3), (4).

Specifically, we consider a square well with constant depth but lateral driving, i.e., with the positions of its walls depending on time in some periodic but otherwise arbitrary manner (fig. 1a),

$$V(x, t) = -V_0 \left[\Theta(x - x_-(t)) - \Theta(x - x_+(t)) \right], \quad (1)$$

where $\Theta(x)$ denotes the Heaviside step function and the wall positions $x_{\pm}(t)$ are periodic functions with the same

period T . A lateral driving arises naturally from an AC voltage through a Kramers-Henneberger gauge transformation [30, 31]. A phase shift between the walls, equivalent to an oscillating width of the well, can be motivated, e.g., by a finite propagation time of time-dependent perturbations across the well or by a superposed gate voltage.

We assume two independent harmonic driving forces (“two-parameter driving”) with phase offset ψ (fig. 1b),

$$x_{\pm}(t) = \pm \frac{a}{2} + x_0 \cos(\omega t \pm \psi/2), \quad \omega = 2\pi/T, \quad (2)$$

where a is the width of the well (in all that follows, $a = 2$, while mass will be fixed at $m = 1$), or alternatively (“single-parameter driving”) a parallel motion of both walls (fig. 1c) with the same periodic time dependence $f(t)$,

$$x_{\pm}(t) = \pm \frac{a}{2} + x_0 f(t), \quad f(t+T) = f(t). \quad (3)$$

Symmetries. In periodically driven scattering, the phase of an incoming trajectory relative to the driving constitutes an additional scattering parameter, besides the incoming momentum $p_{\text{in}} = \lim_{t \rightarrow -\infty} m\dot{x}(t)$. It can be defined, e.g., as $\theta = \omega t_{\text{in}} \bmod 2\pi$, with t_{in} the arrival time of the scattered particle, measured by extrapolating its asymptotic incoming trajectory till the origin $x = 0$ [27]. As θ is typically beyond experimental control, directed transport is considered relevant only if averaged over θ . In order to avoid a systematic cancellation due to counterpropagating trajectory pairs related by P: $\mathbf{r} \rightarrow -\mathbf{r}$, $\mathbf{r} = (p, x)$, $\theta \rightarrow -\theta$ (equivalent to $\omega \rightarrow -\omega$ or $t \rightarrow -t$ for harmonic drivings like (2)), we have to break time-reversal invariance (TRI) of the potential. For eq. (2), this is achieved if $\psi \neq 0, \pi$. In eq. (3), it requires a function $f(t)$ without symmetry or antisymmetry, $f(t_{\pm} - t) \neq \pm f(t)$ for reference times t_{\pm} , as would be the case for a harmonic driving. In the sequel, we choose (cf. fig. 1c)

$$f(t) = \cos(\omega t) + \gamma \cos(2\omega t - \phi), \quad \phi \neq 0, \pi/2, \dots \quad (4)$$

For a two-parameter driving, also ψ could be difficult to control. To make sure that currents do not even vanish upon averaging over ψ , one has to exclude the systematic pairing of trajectories related by P and $\psi \rightarrow -\psi$ [27], e.g., by choosing functions for $x_-(t)$ and $x_+(t)$ not connected by any symmetry. By contrast, for an asymmetric single-parameter driving such as (4), this problem does not arise.

A relevant issue in the context of symmetry is the energy distribution of incoming and outgoing trajectories. In order to analyze deterministic transport processes based on irregular scattering, it would suffice to consider individual scattering events at a given energy, without assuming specific distributions in the asymptotic regions or reservoirs to keep them constant. The strongly inelastic scattering envisaged here, however, together with symmetry breaking suggest to have a closer look at this aspect.

If, for example, for a single-parameter driving we choose $\phi = \pi/2 \bmod \pi$ in eq. (4) (such that $f(\pi/2\omega - t) =$

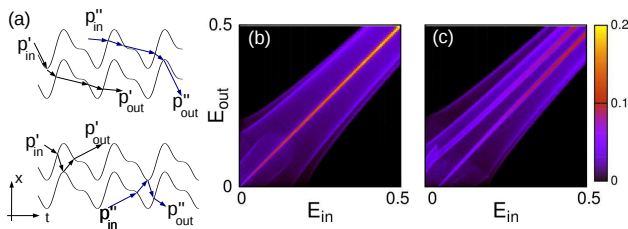


Fig. 2: Symmetry and inelastic scattering. Panel a: Systematic pairing of transmitted (above) and reflected (below) trajectories for single-parameter driving with antisymmetric time dependence $f(\pi/2 - t) = -f(\pi/2 + t)$, eqs. (1), (3), (4) with $\phi = \pi/2$, see text and fig. 1c. b,c: Probability density distributions $\langle d(E_{\text{in}}, E_{\text{out}}) \rangle_{\theta}$ (color code) of outgoing vs. incoming energies for (b) antisymmetric driving as in (a) and (c) asymmetric driving, $\phi = \pi/4$. Other parameter values are $V_0 = 0.75$, $x_0 = 0.1$, $\gamma = 0.2$, $\omega = 1.0$.

$-f(\pi/2\omega + t)$), trajectories come in symmetry-related pairs $\mathbf{r}'(t')$, $\mathbf{r}''(t'')$, with $(p'', x'', t'') = (p', -x', -t')$, see fig. 2a. As a consequence, incoming and outgoing momenta are interchanged within each pair, $p''_{\text{in}} = p'_{\text{out}}$, $p''_{\text{out}} = p'_{\text{in}}$, as are the energies E_{in} , E_{out} . We illustrate the spread of E_{out} vs. E_{in} in fig. 2b,c in terms of the probability density $\langle d(E_{\text{in}}, E_{\text{out}}) \rangle_{\theta}$. In panel (b), the trajectory pairing is clearly reflected in a symmetry of the distribution with respect to the diagonal (the ridge along the diagonal corresponds to elastic processes $E_{\text{in}} = E_{\text{out}}$). It is absent (c) if the antisymmetry of the driving is broken choosing, e.g., $\phi = \pi/4$ in eq. (4).

Therefore, if E_{in} and E_{out} are distributed, say, according to Fermi distributions with the same chemical potential μ and $E'_{\text{in}} < \mu < E'_{\text{out}}$, then the process $E''_{\text{in}} (= E'_{\text{out}}) \rightarrow E''_{\text{out}} (= E'_{\text{in}})$ becomes less probable than $E'_{\text{in}} \rightarrow E'_{\text{out}}$ and a symmetry-induced balance in the reflection probabilities (fig. 2b) from either side is broken for inelastic processes, so that they now contribute to the current. More generally, structures in the energy distribution, even if they occur identically on both sides, can well enable a finite contribution to transport of processes which for homogeneous distributions would be systematically suppressed by some symmetry.

In the present work, we shall not explore this possibility any further. We rather consider transport, in classical as well as quantum calculations, as a function of energy, avoiding averages over this quantity and any assumption as to its distribution or thermalization in reservoirs.

Phase-space structures. In the context of Hamiltonian ratchets, the optimal condition to obtain directed currents is not hard chaos but a mixed dynamics with chaotic and regular regions coexisting in an intricately structured phase space [23, 24]. Chaotic pumps are no exception to this rule. We therefore focus on systems which only marginally pertain to the regime of fully chaotic scattering (defined through the three criteria of (i) the existence of a chaotic repeller in phase space, (ii) self-similar

deflection functions, and (iii) exponential dwell-time distributions [17]).

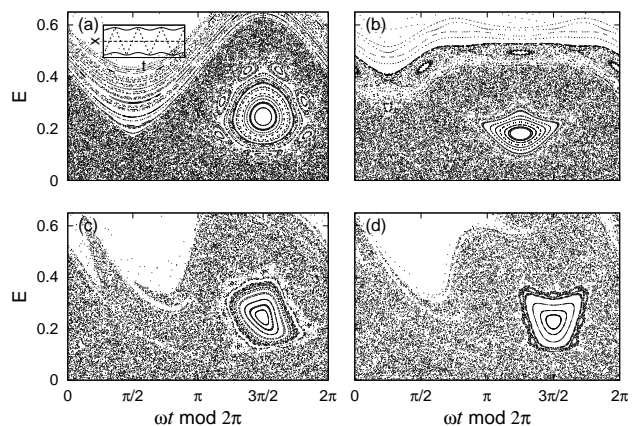


Fig. 3: Poincaré surfaces of section (PSS, defined by $x = 0$, $p > 0$). a,b: two-parameter driving, eqs. (1), (2), c,d: single-parameter driving, eqs. (1), (3), (4); a: with TRI, harmonic driving as in eq. (2) with $\psi = 0$, inset: periodic orbit underlying the prominent regular island, tracing the position $x(t)$ (dotted) between $x_-(t)$ and $x_+(t)$ (full lines); b,c,d: TRI broken with $\psi = \pi/2$ (b), $\gamma = 0.1$ (c,d), $\phi = 0$ (c), $\pi/2$ (d). Other parameter values as in fig. 2. Void areas correspond to trajectories not contained in the initially launched ensemble or intersecting the PSS only a few times in the plotted range.

In fig. 3 we show a set of typical Poincaré surfaces of section, both for a two-parameter, eq. (2) (panels a,b), and a single-parameter driving, eqs. (3), (4) (c,d). In all plots, we observe chaotic regions interspersed with regular islands, characteristic of the KAM scenario [32]. Typically, the regular islands correspond to periodic orbits bound in the scattering region and hence not accessible from outside (see e.g., the inset in panel a). The phase-space structures clearly reflect the presence or absence of spatiotemporal symmetries of the underlying dynamics, as is evident comparing panel a (time-reversal invariant driving) with panels b,c,d (TRI broken).

Directed transport. Moving stepwise from phase-space structures to currents, we shall analyze the relation between scattering and directed transport on two levels: (i) locally, the outcome of individual scattering processes in terms of asymmetries in reflection and transmission from either side, and (ii) globally, currents averaged over the scattering parameters as functions of other pertinent quantities such as driving amplitude and frequency.

Currents are obtained by averaging discrete outcomes (transmission vs. reflection) over suitable parameters, e.g., the phase θ between incoming trajectory and driving force,

$$\langle I \rangle_{\theta} = \frac{1}{2\pi} \int_0^{2\pi} d\theta [T^{-+}(\theta) + R^{++}(\theta)] - [T^{+-}(\theta) + R^{--}(\theta)] \quad (5)$$

where $T^{\pm,\mp}$, $R^{\pm,\pm}$, denote the probabilities for transmission and reflection, resp., between the asymptotic regions

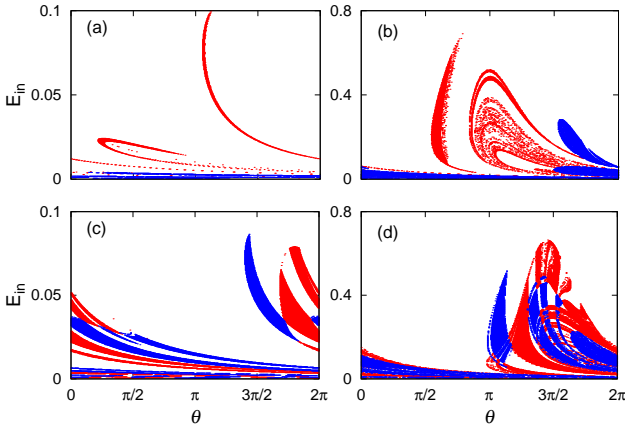


Fig. 4: Directed transport in terms of individual scattering processes in parameter space, weak (panels a,c) vs. strong driving (b,d) for two-parameter, eqs. (1), (2), (panels a,b) and single-parameter driving, eqs. (1), (3), (4) (c,d). Parameter values are $V_0 = 0.75$, $x_0 = 0.05$ (a,c), 0.4 (b,d), $\omega = 1.0$, $\psi = \pi/2$ (a,b), $\gamma = 0.1$, $\phi = \pi/4$ (c,d). Color code: transmission $l \rightarrow r$ and reflection $r \rightarrow r$ blue, transmission $r \rightarrow l$ and reflection $l \rightarrow l$ red, else white.

$x \rightarrow \pm\infty$. The familiar left-right symmetry of transmission and reflection probabilities is generally broken in the absence of a corresponding spatio-temporal invariance of the Hamiltonian, so that, e.g., reflection from left to left can coincide with transmission from right to left at otherwise identical parameter values. We analyze the resulting directed transport “locally in phase space” in fig. 4, contrasting low (panels a,c) with high driving amplitude (b,d). Asymmetric scattering that contributes to directed currents, i.e., exit to the left (right), irrespective of the incoming direction, is labeled red (blue), neutral scattering (same outcome from both sides) white. The emerging structures reflect the relative amount of asymmetric scattering processes as well as the complexity of the underlying phase space, forming fractals analogous to self-similar basin boundaries in dissipative chaotic dynamics [32].

Evidence for directed transport is provided in fig. 5, comparing the dependence of the current on the incoming energy for various values of strength (a) and frequency ω (b) of the driving. As a general tendency, it increases with both parameters but saturates as the period of the driving approaches the time of flight through the scattering region, confirming our expectation that the mixed character of the dynamics plays a decisive rôle for current generation. This is also consistent with the fact that currents vanish for sufficiently high energy: For $E_{\text{in}} \gg V_0$, trajectories belong to the regular part of phase space corresponding to quasi-free motion, cf. fig. 3, hence are always transmitted. At lower energies, current sets in as the first trajectories are reflected for one of the incoming directions and reduces again as the same begins to occur also for the opposite direction. Superposed on these main trends, we observe frequent sign changes. The corresponding sensitive depen-

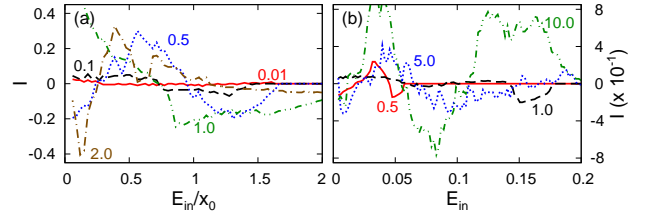


Fig. 5: Average currents as functions of various parameters. Single-parameter driving, eqs. (1), (3), (4). Panel a: current vs. initial energy for different driving amplitudes, $x_0 = 0.01$ (full red line), 0.1 (dashed, black), 0.5 (dotted, blue), 1.0 (dash-double dotted, green), 2.0 (dash-dotted, brown). Other parameter values are $\gamma = 0.1 \times x_0$, $\phi = \pi/2$, $\omega = 1.0$. Panel b: current vs. initial energy for different driving frequencies $\omega = 0.5$ (full line, red), 1.0 (dashed, black), 5.0 (dotted, blue), 10.0 (dash-double-dotted, green). Other parameters are $V_0 = 0.75$, $x_0 = 0.1$, $\gamma = 0.1$, $\phi = \pi/2$.

dence on the parameters has been seen in similar models as well [27, 29] and suggests the possibility of a fine tuning of the current.

It is evident from figs. 4a,c and 5a that even relatively weak driving (and symmetry breaking, not shown) is sufficient to achieve substantial transport. Conversely, this indicates that it will even be difficult to avoid current generation due to small asymmetries in a real experimental setup.

Quantizing chaotic pumps. –

Floquet scattering theory. Scattering at time-dependent potentials is generally inelastic so that standard quantum scattering theory no longer applies. If the driving is periodic, however, large parts of that familiar setting remain intact. A rigorous framework for the treatment of periodically time-dependent quantum systems is provided by Floquet theory [33–35], worked out for scattering systems in Refs. [36, 37]. We here only summarize a few facts directly relevant for us:

- In periodically driven scattering, energy remains conserved mod $\hbar\omega$, the photon energy associated to the periodic driving. For incoming and outgoing asymptotic energies this means

$$E_{\text{in/out}}(\alpha, n_{\text{in/out}}) = \epsilon_\alpha + n_{\text{in/out}}\hbar\omega, \quad (6)$$

where ϵ_α is the *quasienergy* pertaining to a *Floquet eigenstate* α and $n_{\text{in/out}}$ enumerate incoming (outgoing) discrete *Floquet channels*. As a consequence, the total energy difference is $E_{\text{out}} - E_{\text{in}} = m\hbar\omega$, $m = n_{\text{out}} - n_{\text{in}}$ counting the total number of photons gained or lost.

- The time evolution can be composed as a concatenation of discrete steps of duration T generated by the unitary Floquet operator

$$\hat{U}_F = \mathcal{T} \exp \left[-\frac{i}{\hbar} \int_0^T dt \hat{H}(t) \right], \quad (7)$$

where $\hat{H}(t)$ is the Hamiltonian and \mathcal{T} effects time ordering. They give rise to a *discrete* dynamical group, reducing numerical simulations of wavepacket scattering to repeated applications of \hat{U}_F [36, 37].

- The “on-quasienergy-shell” scattering matrix $S_{n,n'}(\epsilon)$ [36, 37] is also organized in terms of Floquet channels n, n' . For one-dimensional scattering systems, it consists of four blocks $S^{\sigma\tau}$, $\sigma, \tau = - (+)$ denoting the left (right) terminal. Accordingly, we define partial transmission and reflection probabilities as

$$T_{n-n'}^{\sigma,-\sigma}(\epsilon + n'\hbar\omega) = |S_{n,n'}^{\sigma,-\sigma}(\epsilon)|^2, \quad (8)$$

$$R_{n-n'}^{\sigma,\sigma}(\epsilon + n'\hbar\omega) = |S_{n,n'}^{\sigma,\sigma}(\epsilon)|^2, \quad (9)$$

and the corresponding total quantities as

$$T_{\text{tot}}^{\sigma,-\sigma}(\epsilon) = \sum_{l=-\infty}^{\infty} T_l^{\sigma,-\sigma}(\epsilon), \quad R_{\text{tot}}^{\sigma,\sigma}(\epsilon) = \sum_{l=-\infty}^{\infty} R_l^{\sigma,\sigma}(\epsilon). \quad (10)$$

Numerical methods. The matrix elements $S_{n,n'}^{\sigma,\tau}(\epsilon)$, as basic input to further evaluation of currents etc. are determined numerically by wavepacket scattering: An initially free wavepacket $|\psi_i^\sigma\rangle$ at a well-defined wavenumber $k_0(\epsilon) = \sqrt{2m\epsilon}/\hbar$ is propagated stroboscopically through the scattering region by repeated application of \hat{U}_F . Once the occupation probability within the interaction region (cf. the integral on the r.h.s. of eq.(13)) has decayed to below some threshold value, the final wavepacket $|\psi_f^\sigma\rangle$ is decomposed into Floquet channels at $k_n(\epsilon) = \sqrt{2m(\epsilon + n\hbar\omega)}/\hbar$, cf. eq. (6), to determine the scattering matrix elements $S_{0,n}^{\sigma,-\sigma} = k_0(\epsilon)\psi_f^{-\sigma}(k_n(\epsilon))/k_n(\epsilon)\psi_i^\sigma(k_0(\epsilon))$. The Floquet operator as main ingredient is most efficiently calculated by the (t, t') method [38].

Spurious interferences between the reflected and the transmitted wavepacket can occur if periodic boundary conditions are imposed at the ends of the finite spatial box underlying the propagation procedure. To prevent them, we employ absorbing boundaries instead. Specifically, the so-called Smooth Exterior Scaling Complex Absorbing Potentials (SES-CAPs [39]), while cumbersome to handle numerically, keep complications due to the corresponding non-Hermitian terms in the Hamiltonian at a minimum, i.e., they are energy independent and leave the physical potential unscaled.

Quantum transport. In order to make contact with the adiabatic approach to pumping and to demonstrate the strongly nonadiabatic character of chaotic pumps, we compare in fig. 6a numerical results for the two-parameter model (2) with the predictions of the adiabatic scattering approach based on the Berry phase [3] (for single-parameter driving, adiabatic transport vanishes identically): For a system with a single degree of freedom, two contacts (left, right), and two independently driven pa-

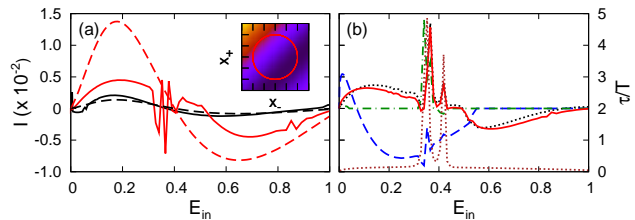


Fig. 6: Quantum current as a function of initial energy. Panel a: Floquet approach (full lines) compared with adiabatic theory, eqs. (11), (12) (dashed) for slow (black, $\omega = 0.1$) vs. fast (red, $\omega = 1.0$) two-parameter driving, eqs. (1), (2). Inset: Parameter cycle in (x_-, x_+) -space (bold red line) and fictitious magnetic field $B(x_-, x_+)$, eq. (12) at $E = 0.45$, underlying the adiabatic approximation (color code: from black, $B < 0$, through red, $B = 0$, through yellow, $B > 0$). Panel b: Total current for single-parameter driving, eqs. (1), (3), (4), with $\omega = 1.0$, $\phi = \pi/2$ (full line, red), Floquet currents in the elastic and first and second inelastic channels, $n = 0, 1, 2$ (dotted black, dot-dashed green, and dashed blue lines, resp., the latter two amplified by factors 10 and 5×10^2 , resp.), and dwell time, eq. (13) (short-dashed brown, rightmost ordinate). Other parameters are $V_0 = 0.75$, $x_0 = 0.1$, $\hbar = 0.5$.

rameters $\xi_1(t)$, $\xi_2(t)$, the probability current (charge current in units of e) through the device is

$$I_{\text{tot}}(E) = \frac{-i\omega}{4\pi^2} \int_A d^2\xi B(\xi, E). \quad (11)$$

Here, A is the area in parameter space enclosed by the path $\xi(t) = (\xi_1(t), \xi_2(t))$ (cf. inset in fig. 6a), penetrated by the “magnetic field”

$$B(\xi, E) = \left[\partial_2 S_{\text{tot}}(E) \partial_1 S_{\text{tot}}^\dagger(E) - \partial_1 S_{\text{tot}}(E) \partial_2 S_{\text{tot}}^\dagger(E) \right]^{++}, \quad (12)$$

where $S_{\text{tot}}(E)$ denotes the (2×2) -matrix $\sum_{n,n'} S_{n,n'}^{\sigma\tau}(E)$, $\partial_i = \partial/\partial\xi_i$.

Fig. 6a contrasts the total current obtained in the Floquet approach (full lines) with the adiabatic approximation (11) (broken). While for slow driving (black, $\omega = 0.1$), we find appreciable agreement, they deviate drastically for fast driving (red, $\omega = 1.0$), indicating that strongly nonlinear transport mechanisms are involved.

Adiabatic theory fails for single-parameter pumps, featured in fig. 6b. We decompose the total current (full line) in Floquet channels (dashed). Although the main contribution comes from the elastic channel ($n = 0$), inelastic scattering ($n = 1, 2$) is also present. Each component, corresponding to a multiphoton process involving the loss or gain of n driving-field photons, scales roughly as ω^n . Sharp resonances in the partial and total currents coincide largely with peaks in the dwell time (dotted brown), measured as the fraction of the wavepacket inside the interaction region summed over stroboscopic time [26],

$$\tau = T \sum_{j=-\infty}^{\infty} \int_{-a/2-x_0}^{a/2+x_0} dx |\psi(x, jT)|^2. \quad (13)$$

Conclusion. – Pumping in the non-adiabatic regime of fast and strong driving, where effects of nonlinear classical dynamics become important, remains largely unexplored. As a first survey into this realm, on the classical as well as the quantum level, we have studied directed transport induced by irregular scattering. In particular, we have pointed out and provided evidence for the possibility of generating currents by driving just a single parameter, which manifestly goes beyond the adiabatic approximation. Their sensitive parameter dependence reflects the underlying chaotic dynamics and suggests to be harnished for control purposes. The corresponding quantum transport has been studied in the framework of the exact Floquet scattering formalism. We have not been able to go into the numerically very demanding regime of small effective Planck’s constant in order to apply semiclassical methods [40].

Our model has been kept utterly simple, focused on the analysis of chaotic scattering and its impact on directed transport. Several options are conceivable to include more realistic details: Many-particle phenomena like charge blocking, dissipation, decoherence, and finite-temperature energy distributions in the reservoirs are obviously relevant. To be adequately treated, they require sophisticated nonequilibrium methods such as the Keldysh Green function technique [10, 41, 42]. Other directions to extend the model are incorporating internal degrees of freedom such as in particular spin, to enrich the chaotic dynamics and study nonlinear transport in the corresponding current components [29], as well as pumping against a potential gradient.

* * *

We enjoyed inspiring discussions with Doron Cohen and François Leyvraz. TD acknowledges with pleasure the hospitality of Ben Gurion University of the Negev during various stays at Beer-Sheva and financial support by Volkswagenstiftung (grant I/78 235).

REFERENCES

- [1] THOULESS D., *Phys. Rev. B* , **27** (1983) 6083.
- [2] ALTSHULER B. and GLAZMAN L., *Science* , **283** (1999) 1864.
- [3] BROUWER P., *Phys. Rev. B* , **58** (1998) R10135.
- [4] AVRON J., ELGART A., GRAF G. and SADUN L., *Phys. Rev. B* , **62** (2000) R10618.
- [5] MOSKALETS M. and BÜTTIKER M., *Phys. Rev. B* , **66** (2002) 205320.
- [6] COHEN D., *Phys. Rev. B* , **68** (2003) 155303.
- [7] OOSTERKAMP T., KOUWENHOVEN L., KOOLEN A., VAN DER VAART N. and HARMANS C., *Phys. Rev. Lett.* , **78** (1997) 1536.
- [8] BLICK R., VAN DER WEIDE D., HAUG R. and EBERL K., *Phys. Rev. Lett.* , **81** (1998) 689.
- [9] PRADA E., SAN-JOSE P. and SCHOMERUS H., *Phys. Rev. B* , **80** (2009) 245414.
- [10] GU Y., YANG Y. H., WANG J. and CHAN K. S., *J. Phys.: Cond. Mat.* , **21** (2009) 405301.
- [11] TORRES L. E. F. F., *Phys. Rev. B* , **72** (2005) 245339.
- [12] MAHMOODIAN M. M., BRAGINSKY L. S. and ENTIN M. V., *Phys. Rev. B* , **74** (2006) 125317.
- [13] AGARWAL A. and SEN D., *Phys. Rev. B* , **76** (2007) 235316.
- [14] COHEN D., KOTTOS T. and SCHANZ H., *Phys. Rev. E* , **71** (2005) 035202(R).
- [15] SELA I. and COHEN D., *J. Phys. A: Math. Gen.* , **39** (2006) 3575.
- [16] HOFFMANN S., HOFMANN M., KIRA M. and KOCH S., *Semicond. Sci. Technol.* , **20** (2005) S205.
- [17] SMLANSKY U., in *Chaos and Quantum Physics*, edited by GIANNONI M.-J., VOROS A. and ZINN-JUSTIN J., Vol. LII of *Les Houches Lectures* (North-Holland–Elsevier, Amsterdam) 1992 p. 371.
- [18] BENET L., TRAUTMANN D. and SELIGMAN T., *Cel. Mech. Dyn. Astron.* , **66** (1997) 203.
- [19] NOID D., GRAY S. and RICE S., *J. Chem. Phys.* , **84** (1986) 2649.
- [20] BRUMER P. and SHAPIRO M., *Adv. Chem. Phys.* , **70** (1988) 365.
- [21] GASPARD P. and RICE S., *J. Chem. Phys.* , **90** (1989) 2225; *ibid.* 2242; *ibid.* 2255.
- [22] REIMANN P., *Phys. Rep.* , **361** (2002) 57.
- [23] SCHANZ H., OTTO M.-F., KETZMERICK R. and DITTRICH T., *Phys. Rev. Lett.* , **87** (2001) 070601.
- [24] SCHANZ H., DITTRICH T. and KETZMERICK R., *Phys. Rev. E* , **71** (2005) 026228.
- [25] HENSELER M., DITTRICH T. and RICHTER K., *Europhys. Lett.* , **49** (2000) 289.
- [26] HENSELER M., DITTRICH T. and RICHTER K., *Phys. Rev. E* , **64** (2001) 046218.
- [27] DITTRICH T., GUTIÉRREZ M. and SINUCO G., *Physica A* , **327** (2003) 145.
- [28] FLACH S., YEVTUSHENKO O. and ZOLOTARYUK Y., *Phys. Rev. Lett.* , **84** (2000) 2358.
- [29] DITTRICH T. and DUBEIBE F., *J. Phys. A: Math. Theor.* , **41** (2008) 265102.
- [30] KRAMERS H., *Collected Scientific Papers* (North-Holland, Amsterdam) 1956.
- [31] HENNEBERGER W., *Phys. Rev. Lett.* , **21** (1958) 838.
- [32] OTT E., *Chaos in dynamical systems* (Cambridge University Press, Cambridge (UK)) 1993.
- [33] SAMBE H., *Phys. Rev. A* , **7** (1973) 2203.
- [34] HOWLAND J., *Indiana Univ. Math. J.* , **28** (1979) 471.
- [35] YAJIMA K., *J. Math. Soc. Jpn.* , **29** (1979) 729.
- [36] ŠEBA P., *Phys. Rev. E* , **47** (1993) 3870.
- [37] ŠEBA P. and GERWINSKI P., *Phys. Rev. E* , **50** (1994) 3615.
- [38] PESKIN U. and MOISEYEV N., *J. Chem. Phys.* , **99** (1993) 4590.
- [39] SHEMER O., BRISKER D. and MOISEYEV N., *Phys. Rev. A* , **71** (2005) 032716.
- [40] RICHTER K. and SIEBER M., *Phys. Rev. Lett.* , **89** (2002) 206801.
- [41] WANG B., WANG J. and GUO H., *Phys. Rev. B* , **65** (2002) 073306.
- [42] ARRACHEA L. and MOSKALETS M., *Phys. Rev. B* , **74** (2006) 245322.